Ticks and Tick-borne Diseases 10 (2019) 787–797

Contents lists available at ScienceDirect

Ticks and Tick-borne Diseases

journal homepage: www.elsevier.com/locate/ttbdis

Original article

Tick Gené's organ engagement in lipid metabolism revealed by a combined transcriptomic and proteomic approach

Marina Amaral Xavier[a,b], Lucas Tirloni[c], Antonio F.M. Pinto[d,e], Jolene K. Diedrich[d], John R. Yates III[d], Sergio Gonzales[f], Marisa Farber[f], Itabajara da Silva Vaz Junior[a,g], Carlos Termignoni[a,b,*]

[a] Centro de Biotecnologia, Universidade Federal do Rio Grande do Sul, Porto Alegre, RS, Brazil
[b] Departamento de Bioquímica, Universidade Federal do Rio Grande do Sul, Porto Alegre, RS, Brazil
[c] Vector Biology Section, Laboratory of Malaria and Vector Research, National Institute of Allergy and Infectious Disease, Rockville, MD, United States
[d] Department of Molecular Medicine, The Scripps Research Institute, La Jolla, CA, United States
[e] Clayton Foundation Peptide Biology Lab, Salk Institute for Biological Studies, La Jolla, CA, United States
[f] Instituto de Biotecnología, Instituto Nacional de Tecnología Agropecuaria, Hurlingham, BA, Argentina
[g] Faculdade de Veterinária, Universidade Federal do Rio Grande do Sul, Porto Alegre, RS, Brazil

ARTICLE INFO

Keywords:
Gené's organ
Egg wax
Lipid gland
Tick
Proteome
Transcriptome

ABSTRACT

Lipids play key roles in arthropod metabolism. In ticks, these biomolecules are transported from fat body to other organs, such as ovary and Gené's organ. Gené's organ, an apparatus found exclusively in female ticks, secretes a protective wax coat onto the egg surface, increasing egg viability in the environment due to waterproof, cohesive, and antimicrobial properties. In this work, a combined transcriptomic and proteomic approach shows that Gené's organ not solely secrets compounds taken up from the hemolymph, but is actively engaged in synthesis, modification, and oxidation of lipids. Gené's organ was analyzed at two distinct stages: 1) when ticks detach from host by the end of hematophagous phase, and 2) during egg-laying. Data show that Gené's organ undergoes a maturation process before the onset of oviposition, in preparation for its role during egg-laying. Because it deals with a wax-secreting organ, the study focused on lipid metabolism, examining a full machinery to synthesize, modify, and oxidize fatty acids. Proteins involved in sterol modification, transport, and degradation were also addressed. In addition to highlighting Gené's organ importance in tick reproductive physiology, the results reveal proteins and pathways crucial to egg wax secretion, and consequently, egg development in the environment. Tools targeting these molecules and pathways would impair egg viability in the environment, and therefore have the potential to be developed into novel tick control methods.

1. Introduction

In arthropods, lipids play key roles as chemical messengers (hormones and pheromones), as energy source and storage, in constituting cellular membranes, and in egg production, laying and viability (Canavoso et al., 2001; Lees and Beament, 1948; Ryan and van der Horst, 2000). Like for most phenomena in arthropod physiology, the knowledge about lipid metabolism is mainly based on and extrapolated from studies on insects. Digestion and absorption of lipids from the diet occurs in the midgut, but lipid metabolism takes place mostly in the fat body, an organ that functions similarly to an adipose tissue and liver (Arrese and Soulages, 2010; Majerowicz and Gondim, 2013). In ticks, after metabolized in the fat body, lipids are transported through the hemolymph to other organs, such as ovary and Gené's organ (GO) (Kluck et al., 2018).

The success of tick egg development in the environment relies on GO activity (Lees and Beament, 1948). This organ is present only in female ticks and covers the eggshell with a waxy layer immediately after each egg is released from the genital aperture. The vestibulum vaginae prolapses from the genital aperture and hands over each egg to the horns of GO (Sieberz and Gothe, 2000). In addition to protecting the egg from environmental conditions of humidity and temperature, the wax deposited on the surface makes egg development feasible due to its antimicrobial (Arrieta et al., 2006; De Lima-Netto et al., 2012; Esteves et al., 2009; Potterat et al., 1997; Yu et al., 2012; Zimmer et al., 2013ab) and waterproof (Lees and Beament, 1948) properties. The wax

* Corresponding author.
E-mail address: trmgn@cbiot.ufrgs.br (C. Termignoni).

https://doi.org/10.1016/j.ttbdis.2019.03.013
Received 7 January 2019; Received in revised form 27 February 2019; Accepted 15 March 2019
Available online 20 March 2019
1877-959X/

stickiness also promotes egg clustering, reducing the total surface exposure and possibly enhancing the protective properties (Booth, 1992; Lees and Beament, 1948).

The study of GO has focused on its morphology and histology (Booth, 1989; Booth et al., 1985; dos Santos et al., 2018; El Shoura, 1988, 1987; Kakuda et al., 1992; Schöl et al., 2001), *modus operandi* (Edelmann and Gothe, 2000; Sieberz and Gothe, 2000), and on wax content and properties (Booth, 1989; Yu et al., 2012). The wax is mainly composed of long-chain alkanes, fatty acid esters (Booth, 1992), cholesterol ester, free cholesterol and fatty acids (Yu et al., 2012). Other lipids present at lower abundance are phosphatidylcholine, sphingomyelin, triglyceride, monoglyceride, phosphatidylethanolamine and phosphatidylserine (Yu et al., 2012).

Histological studies have shown an enrichment of endoplasmic reticulum and Golgi apparatus in GO cells (Booth, 1989; dos Santos et al., 2018; Kakuda et al., 1995), supporting the hypothesis that GO is involved in synthetic pathways and not just in transferring material from the hemolymph to the egg surface. Evidence that GO is involved in lipid synthesis has been presented by studies showing the incorporation of ^{14}C-1-acetate into GO secretory glands and egg wax (Booth, 1992). In contrast, histological observations of invagination structures on the basal plasma membrane of GO secretory cells have led authors to hypothesize that GO is not a synthesis organ, but secretes molecules provided by the hemolymph (dos Santos et al., 2018; Kakuda et al., 1995).

In order to investigate the development and function of *Rhipicephalus microplus* GO, transcriptomic and proteomic approaches were used to compare the molecular content of GO in two stages: by the end of hematophagous phase and during egg-laying. Data presented here show that GO is functional in synthesizing and modifying lipid content, not only secreting it. Additionally, a survey of all genes being expressed in GO in two stages of tick development is presented.

2. Material and methods

2.1. Ethics statement

This research was conducted according to the ethic and methodological guidance in agreement with the International and National Directives and Norms by Animal Experimentation Ethics Committee of Universidade Federal do Rio Grande do Sul (UFRGS) (project n° 31,518).

2.2. Ticks

Ticks obtained from a laboratory colony of *R. microplus* (Porto Alegre strain, Porto Alegre, Brazil) were reared on Hereford cattle (*Bos taurus taurus*) brought from a naturally tick-free area and maintained in insulated pens (Reck et al., 2009). A calf was infested with 15-day-old larvae, and ticks naturally detached from host were collected after completing the hematophagy period (around 22 days). Fifty females ranging between 230 and 270 mg were placed in two groups for GO extraction. The first group consisted of females that detached from host and were dissected within 24 h (group DET n = 25); the second group consisted of females kept in an incubator for egg-laying (28 °C and 85% relative humidity) and dissected in the second day of oviposition, around 5 days after detaching from host (group OVP n = 25).

2.3. Gené's organ dissection, total RNA and protein extraction

Firstly, ticks were washed in 70% ethanol for 10 min and then air-dried. After dissection, GO were gently washed in nuclease-free phosphate-buffered saline (150 mM sodium phosphate monobasic and 10 mM sodium chloride, pH 6.7), and immediately transferred to TRIzol® reagent (Thermo Fisher Scientific). Total RNA and protein were isolated according to manufacturer's specifications. Dissected GO from each group were divided in three samples for total RNA and protein extraction: two samples containing GO from 10 ticks each, and one sample containing GO from five ticks. The three RNA samples were used to construct three cDNA libraries submitted to RNA-seq. Protein extracts from the two 10-tick samples were analyzed by LC−MS/MS.

2.4. RNA-seq and bioinformatic analysis

The construction of paired-end cDNA libraries was performed using TruSeq RNA Library Prep Kit, according to manufacturer's specifications. Samples were tagged with specific barcodes and paired-end reads were sequenced using an Illumina MiSeq platform (Illumina, San Diego, CA, USA) at Unidad de Genómica/Nodo Plataforma de Genómica CATG facility (Hurlingham, BA, Argentina).

Raw data was evaluated using FastQC (https://www.bioinformatics.babraham.ac.uk/projects/fastqc/), trimmed using Trimmomatic (Bolger et al., 2014), and the overlapping reads were combined using FLASh tool (Magoč and Salzberg, 2011). The *de novo* assembly was performed using Trinity (Grabherr et al., 2011) (*k-mer* size of 31 and sequence length of 500 nucleotides) using reads generated in this study, along with *R. microplus* GO transcriptome raw data available on Sequence Read Archive (SRA) (BioProject ID PRJNA288687) (Tidwell, 2015). From each transcript, the six potential translational frames of coding sequences (CDS) (deduced CDS) were extracted, provided they encoded a minimum of 67 amino acids. In order to retain only the transcripts generated by the current study, reads from each library (three from DET group and three from OVP group) were mapped to the deduced CDS (> 67 amino acids) using Bowtie2 (Langmead and Salzberg, 2012). Then, eXpress (Roberts and Pachter, 2013) and edgeR (Robinson et al., 2009) were used to remove low-expression contigs, retaining contigs fulfilling the following criteria: counts per million (CPM) > 1 and presence in at least two out of the three libraries.

The following methodology was performed as previously described by (Karim et al., 2011; Ribeiro et al., 2016). In order to select which deduced CDS were putative CDS, the resulting contigs were concatenated and the redundancy removed. Then, putative CDS were extracted based on similarity to protein sequences available in public databases, using BLASTp. Sequences matching 50% or more of the length of proteins in the databases had their putative CDS automatically extracted by a program written in Visual Basic.

Reads from each library were then mapped to the deduced CDS, using BLASTn with word size of 25, 1 gap allowed, and identity ≥97% required. Up to five matches were allowed provided scores were the same as the highest score. An average of reads per contig was calculated for each group (DET or OVP). A resulting spreadsheet with the average number of reads per contig per group was used to calculate fragments per kilobase million (FPKM). FPKM was calculated for each contig in the spreadsheet using the formula:

$$\frac{number\ of\ reads}{(sequence\ lenght\ in\ kilobases \times total\ reads\ per\ million\ in\ the\ group}$$

Filtered reads were submitted to differential expression analysis using the package edgeR (Robinson et al., 2009). Statistically significant differentially expressed genes (DE) are presented according to treatment (DET and OVP) using counts per million (CPM) ≥1 and false discovery rate < 0.05 (5% FDR). Results are displayed as volcano plots.

Functional annotation of coding sequences was performed using an automated annotation tool based on a vocabulary of nearly 250 words found in matches to different non-redundant protein databases of NCBI (Karim et al., 2011). Additional manual annotation was made as required. In addition, reverse position-specific BLAST (Reverse PSI-BLAST) (Altschul et al., 1997) was used to search for conserved protein domains in the CDD database (Marchler-Bauer et al., 2002). In the last step, coding sequences were categorized according to function and/or protein families.

Raw data obtained in this work were deposited in the National

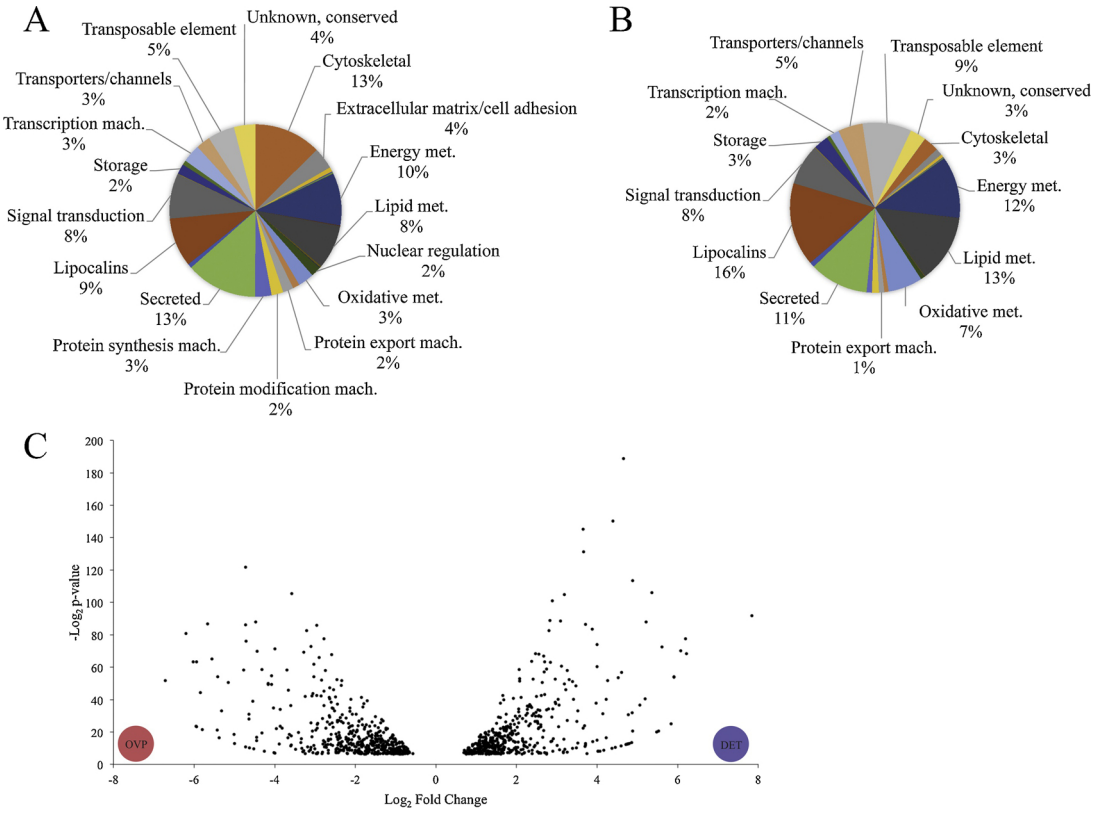

Fig. 1. Gené's organ (GO) coding sequences (CDS) profile before and during egg-laying. GO was obtained from ticks in two developmental stages: (A) within 24 h of detachment from host (DET group), and (B) in the second day of oviposition (OVP group), i.e. around 5 days after detachment. CDS are categorized according to biological function of the translated protein. Categories' FPKM (fragments per kilobase million) is presented as percentage, normalized by the total FPKM of each group, in order to represent the total amount of each category in each GO stage. (C) Volcano plot displaying common CDS that were differentially expressed between DET and OVP groups, based on fold change (FC) (y-axis) and counts per million (CPM) (x-axis). Dots in y-axis positive side are from DET group, while dots in y-axis negative side are from OVP group. mach = machinery; met = metabolism.

Table 1
Overview of *Rhipicephalus microplus* Gené's organ transcriptome data.

	DET group	OVP group
Reads (150 nt)	2.1–2.2 million	2.3–2.4 million
Assembly	97,527	
Deduced CDS > 67aa	380,223	
Mapping and filtering (CPM > 1) deduced CDS	40,293	48,602
Non-redundant deduced CDS	60,943	
Putative CDS (average 321 nt)	3869	
Functional annotation of putative CDS	1285	

CDS = coding sequence.

Center for Biotechnology Information (NCBI) Sequence Read Archives (SRA) under the accession SRR7876048 and SRR7876049 ((these are linked to BioSample SAMN02463642 of the Bioproject PRJNA232001). Functional annotated contigs were deposited in Transcriptome Shotgun Assembly (TSA) project at DDBJ/EMBL/GenBank under the accession GGXY00000000. The version described in this paper is the first version, GGXY01000000.

2.5. High-performance liquid chromatography coupled with tandem mass spectrometry (LC–MS/MS) and data analysis

The four samples described in section 2.3 were analyzed by LC–MS/MS in triplicates. Subsequently to extraction (section 2.3), protein concentration was measured using BCA Protein Assay Reagent Kit (Thermo Scientific Pierce), following the manufacturer's recommendations. Proteins were precipitated using methanol/chloroform method (Wessel and Flügge, 1984). Dried pellets were dissolved in 8 M urea/100 mM Tris, pH 8.5, reduced with 5 mM TCEP, alkylated with 25 mM iodoacetamide, and digested overnight at 37 °C using trypsin at a final ratio of 1:20 (w/w; enzyme: substrate) in 2 M urea/100 mM Tris pH 8.5, 1 mM $CaCl_2$ buffer. Digestion reactions, at a final concentration of 1 µg/µL, were quenched with formic acid (5% final concentration), and debris were removed by centrifugation at 17,000 x g for 5 min at 4 °C.

Reversed-phase pre-columns were prepared in 250 µm ID/360 µm OD capillary with a Kasil frit at one end. Pre-columns were packed in-house with 2 cm of 5 µm ODS-AQ C18 from particle slurries in methanol. Analytical reversed-phase columns were prepared by pulling a 100 µm ID/360 µm OD silica capillary to a 5-µm ID tip and packing 20 cm of the same particles directly behind the pulled tip. Reversed-phase pre-columns and analytical columns were connected using a zero-dead volume union.

Peptide mixtures were analyzed by nanoflow LC—MS using an Easy NanoLC II coupled to a Q Exactive mass spectrometer (Thermo Scientific). Peptides eluted from the analytical column were electrosprayed directly into the mass spectrometer. Solutions A and B consisted of 5% acetonitrile/0.1% formic acid and 80% acetonitrile/0.1% formic acid, respectively. The flow rate was set to 400 nL/min. Protein samples from each group (1.5 µg per injection) were submitted to 155-min chromatographic runs, as follows: 1–10 % B in 10 min, 10–40 % B

Table 2
Functional categorization of *R. microplus* GO CDSs before and during egg-laying.

Functional categories	DET			OVP		
	Number of CDS	Number of reads	Relative abundance of reads (%)	Number of CDS	Number of reads	Relative abundance of reads (%)
Amino acid metabolism	6	113	0.16	6	109	0.11
Bacterial	3	35	0.05	3	54	0.05
Carbohydrate metabolism	11	147	0.21	11	124	0.12
Cytoskeletal	80	6932	9.98	79	2251	2.24
Energy metabolism	4	7532	10.85	4	19,195	19.12
Extracellular matrix/cell adhesion	90	2765	3.98	85	1194	1.19
Immunity	13	377	0.54	13	334	0.33
Intermediate metabolism	4	63	0.09	4	22	0.02
Lipid metabolism	37	6687	9.63	36	14,891	14.84
Lipocalins	2	8802	12.67	2	19,021	18.95
Nuclear export	9	131	0.19	9	75	0.07
Nuclear regulation	63	1291	1.86	62	750	0.75
Nucleotide metabolism	12	209	0.30	12	128	0.13
Oxidative metabolism	14	1985	2.86	15	5303	5.28
Proteasome machinery	48	745	1.07	48	659	0.66
Protein export machinery	37	1210	1.74	40	851	0.85
Protein modification machinery	41	1616	2.33	41	1028	1.02
Protein synthesis machinery	20	1427	2.05	20	619	0.62
Proteinase inhibitor	2	367	0.53	2	557	0.55
Secreted	97	7559	10.88	98	6391	6.37
Signal transduction	165	4907	7.07	168	5934	5.91
Signal transduction, apoptosis	6	73	0.11	6	97	0.10
Storage	6	934	1.34	6	1737	1.73
Transcription factor	29	537	0.77	29	539	0.54
Transcription machinery	94	3314	4.77	93	2774	2.76
Transporters/channels	44	2109	3.04	46	5343	5.32
Transposable element	182	3978	5.73	190	7658	7.63
Unknown, conserved	101	3605	5.19	99	2739	2.73
Total	1,220	69,450	100	1,227	100,377	100

in 100 min, 40–50 % B in 10 min, and 50–90 % B in 10 min. The column was held at 90% B for 10 min, and re-equilibrated in 1% B prior to next injection.

The mass spectrometer was operated in a data-dependent mode, collecting a full MS scan from 400 to 1200 *m/z* at 70,000 resolution and an automatic gain control (AGC) target of 1×10^6. The 10 most abundant ions per scan were selected for MS/MS at 17,500 resolution, AGC target of 2×10^5, and an underfill ratio of 0.1%. Maximum fill times were 20 ms and 120 ms for MS and MS/MS scans, respectively, with dynamic exclusion of 15 s. Normalized collision energy was set to 25.

Tandem mass spectra were searched directly from RAW files with Comet (Eng et al., 2013) in the platform PatternLab for Proteomics (Carvalho et al., 2016). Resulting mass spectra were searched against two transcriptomic databases: (i) a local *R. microplus* protein database (Rm-INCT-EM) containing 22,010 sequences previously generated by our research group; and (ii) the predicted amino acid sequences translated from *R. microplus* GO nucleotide sequences presented in the current study. Both deposited data belong to the BioProject ID PRJNA232001 at Transcriptome Shotgun Assembly (TSA) database-GenBank. Search was performed using these non-redundant databases and reverse sequences of all entries, and included all fully-tryptic and half-tryptic peptide candidates. Carbamidomethylation of cysteine was used as static modification. The validity of the peptide spectrum matches (PSMs) generated by COMET was assessed using Search Engine Processor (SEPro) module from PatternLab for Proteomics platform. XCorr, DeltaCN, DeltaMass, ZScore, number of peaks matched, and secondary rank values were used to generate a Bayesian discriminating function. A cut-off score was established to accept an FDR of 1% based on the number of decoys. A minimum sequence length of six residues per peptide was required, and results were post-processed to only accept PSMs with precursor mass error < 10 ppm.

Quantitative analysis was performed using the semi-quantitative method based on normalized spectral abundance factor (NSAF), which was calculated according to (Zybailov et al., 2006). NSAF for a given protein is the number of spectral counts (SpC) identified for that protein, divided by the protein's length (L), divided by the sum of SpC/L of all proteins in the experiment. The following parameters were used to select differentially expressed proteins: proteins were grouped by maximum parsimony, spectral count data were normalized using NSAF values, and two nonzero replicate values were required for each condition (at least two out of three replicates). BH q-value was set at 0.02 (2% FDR). A variable fold-change (FC) cut-off for each individual protein was calculated according to the *t*-test p-value using an F-stringency value automatically optimized using the TFold software. Low-abundance proteins were removed using an L-stringency value of 0.4.

Venn diagram comparing samples from groups DET and OVP were produced in PatternLab for Proteomics software, using proteins present in at least 2 replicates. Volcano plot was generated by a pairwise comparison of DET and OVP using the PatternLab's TFold module.

Protein functional annotation was performed as described above for CDS functional annotation (section 2.4). Finally, proteins were categorized according to function and/or protein families. Eight proteins were identified as contaminants and removed from the final list. Mass spectrometry proteomics data have been deposited in the ProteomeXchange Consortium (Deutsch et al., 2017) via PRIDE (Vizcaíno et al., 2016) partner repository with the dataset identifier PXD011223.

3. Results and discussion

3.1. Gené's organ transcriptome data analysis

In order to evaluate molecular processes involved in GO development, transcription in GO was investigated at two stages: i) at the day of detachment from host (DET) and (ii) at the second day of oviposition (OVP), i.e. around 5 days after detachment (Supplementary Fig. 1).

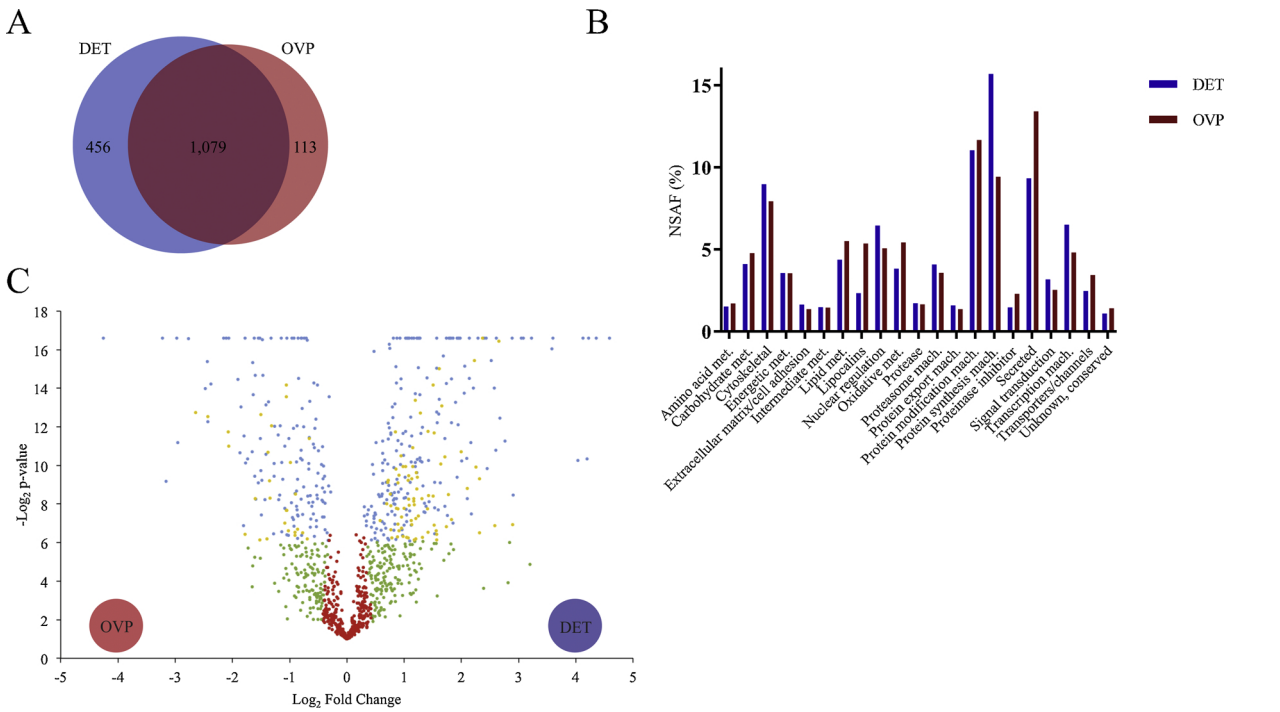

Fig. 2. Comparison of Gené's organ (GO) proteome before and during egg-laying. Protein was obtained from GO in two developmental stages: within 24 h of detachment from host (DET group), and in the second day of oviposition (OVP group), i.e. around 5 days after detachment. (A) Venn diagram displaying the number of proteins found in GO proteome. (B) Identified proteins were categorize according to their biological function. Categories' NSAF (normalized spectral abundance factor) is presented as percentage, normalized by the total NSAF of each group, in order to represent the total amount of each category in each GO stage. (C) Volcano plot displaying common proteins that were differentially abundant between the two stages, based on fold change (FC) (x-axis) versus *t*-test probability (y-axis). Dots in x-axis positive side are from DET group, while dots in x-axis negative side are from OVP group. Blue dots: satisfied both FC and statistical criteria. Yellow dots: filtered out by L-stringency, further experimentation is required to verify if they are indeed differentially abundant. Green dots: satisfied the FC criteria but, most likely, this happened by chance. Red dots: did not meet the FC and p-value criteria. mach = machinery; met = metabolism (For interpretation of the references to colour in this figure legend, the reader is referred to the web version of this article).

R. microplus GO transcriptome in each developmental stage was determined using high throughput RNA-seq. An overview of GO transcriptome data analysis is presented in Table 1. For each library, over 2 million reads were obtained. Reads were assembled in 97,527 transcripts, from which 380,223 deduced coding sequences (CDS) within six translation frames were obtained. Reads from each library were mapped back to these 380,223 deduced CDS, and an expression level threshold (section 2.4) was used to select against low-expression transcripts, which possibly represent assembly artefacts or background expression. After mapping and filtering, 40,293 deduced CDS were obtained for group DET, and 48,602 for group OVP; a total of 60,943 non-redundant deduced CDS were obtained. In order to select which deduced CDS could be putative CDS, sequences were extracted again based on similarity to known proteins on public databases. Through this strategy, 3869 putative proteins with theoretical biological relevance were obtained, of which 1257 were assigned to different functional categories (Table 2 and Supplementary Table S1).

In the DET group, the most abundant (FPKM) coding sequences encode for secreted proteins (13%), proteins related to the cytoskeleton (13%) and energy metabolism (10%) (Fig. 1A). In the OVP group, the most abundant coding sequences represent lipocalins (16%), lipid metabolism (13%), energy metabolism (12%) and secreted proteins (11%) categories (Fig. 1B). The abundance of lipocalins such as histamine-, serotonin- and cholesterol-binding proteins highlights their importance in tick physiology (Beaufays et al., 2008; Neelakanta et al., 2018; Roversi et al., 2017). The relative transcription of cytoskeleton-related proteins was higher in DET group (13%) compared with OVP group (3%), which inversely correlates to the increase in GO size, from unfed females to egg-laying ticks (Schöl et al., 2001). In parallel, the higher relative transcription in OVP group of lipocalin genes (16% versus 9% in DET) and lipid metabolism genes (13% versus 8% in DET) suggest that GO maintains metabolite transport and synthesis and/or modification of lipids during egg-laying.

These results are corroborated by differential gene expression between the groups, which are represented in Fig. 1C and described in detail in Supplementary Table S1. In DET group, the most differentially expressed CDS encode for proteins related to extracellular matrix (e.g. heparan sulfate proteoglycan 2, $\log_2FC = 6$), signal transduction (e.g. low-density lipoprotein receptor, $\log_2FC = 5$), cytoskeleton (e.g. similar to microtubule associated protein, $\log_2FC = 5$), secreted proteins (e.g. mucin-19-like, $\log_2FC = 6$), and transcription machinery. On the other hand, in OVP group, differentially expressed CDS correspond to signal transduction (e.g. protein serine/threonine kinase cdk family, $\log_2FC = 5$), transposable elements (e.g. tick transposon, $\log_2FC = 5$), lipid metabolism (e.g. fatty acyl-CoA elongase, $\log_2FC = 4$), and secreted proteins (e.g. fucolectin tachylectin-4 pentraxin-1 domain protein, $\log_2FC = 3$).

3.2. Gené's organ proteome overview

In addition to the transcriptomic analysis, the proteomic profile of GO was assessed. The complete list of identified proteins is presented in Supplementary Table S2, and a semi-quantitative analysis is shown in Supplementary Table S3.

After filtering out 239 proteins which did not fit the parameters described in section 2.5, and eight proteins corresponding to bovine keratin contaminants, a total of 1648 proteins were identified: 456 are exclusive of DET group, 113 of OVP group, and 1079 are present in both groups (Fig. 2A). Protein functional annotation led to categorization in 29 biological categories (Table 3). The most abundant

Table 3
Functional categorization of *R. microplus* GO proteins before and during egg-laying.

Functional categories	DET		OVP	
	Number of Contigs	Relative NSAF (%)	Number of Contigs	Relative NSAF (%)
Amino acid metabolism	38	1.5	31	1.7
Antimicrobial	1	0.0	2	0.0
Carbohydrate metabolism	63	4.1	44	4.8
Cytoskeletal	77	9.0	63	7.9
Energetic metabolism	68	3.6	56	3.6
Extracellular matrix/cell adhesion	50	1.6	40	1.4
Immunity	20	0.6	14	0.7
Intermediate metabolism	26	1.5	24	1.5
Lipid metabolism	97	4.4	86	5.5
Lipocalins	9	2.3	8	5.4
Nuclear export	11	0.1	4	0.0
Nuclear regulation	67	6.5	33	5.1
Nucleotide metabolism	32	0.9	16	0.6
Oxidative metabolism	55	3.8	50	5.4
Protease	45	1.7	37	1.7
Proteasome machinery	76	4.1	69	3.6
Protein export machinery	70	1.6	56	1.4
Protein modification machinery	82	11.0	75	11.7
Protein synthesis machinery	208	15.7	143	9.4
Proteinase inhibitor	23	1.5	20	2.3
Secreted	52	9.3	56	13.4
Signal transduction	99	3.2	80	2.5
Signal transduction, apoptosis	13	0.2	9	0.1
Storage	10	0.6	8	0.1
Transcription factor	15	0.9	13	0.5
Transcription machinery	119	6.5	76	4.8
Transporters/channels	68	2.5	48	3.4
Unknown	1	0.0	1	0.1
Unknown, conserved	40	1.1	30	1.4
Total	1,535	100	1,192	100

categories were: protein synthesis machinery (16% and 9% in DET and OVP groups, respectively), protein modification machinery (11% and 12%), secreted proteins (9% and 13%), and cytoskeleton (9% and 8%). Protein categories with abundance higher than 1% are displayed in Fig. 2B.

Among the 1079 proteins in common between the two developmental stages of GO, 342 are significantly different in abundance (blue dots in Fig. 2C). Protein synthesis machinery is more abundant in DET (15% versus 7% in OVP), whereas secreted proteins are more highly represented in OVP (22% versus 16% in DET), as observed also for lipocalins (8% in OVP versus 4% in DET). On the other hand, 633 proteins were found to be present at statistically equivalent abundance between the two GO developmental stages. These proteins are involved in protein synthesis and modification machineries, nuclear regulation, transcription machinery, and cytoskeleton (green and red dots in Fig. 2C). The data suggests that GO maintains a basal state before and during egg-laying, which is focused on the machinery for gene transcription and translation, structural proteins of cytoskeleton, secreted proteins, and lipocalins (Table 2).

Data further show a contrasting profile of proteins present exclusively in DET or OVP group (Fig. 3). In DET group, the majority of proteins belong to protein synthesis machinery (16%), nuclear regulation (10%), transcription machinery (9%), and transporters/channels (9%). In OVP group, the most abundant categories are secreted proteins (17%), transporters/channels (16%), lipid metabolism (13%), and unknown conserved proteins (13%). Thus, besides the basal metabolism observed in both stages, GO shows an activity more directed toward synthesis of molecules before oviposition, whereas during oviposition the activity seems more focused on secretion and transport, as well as metabolism of lipids, the main GO secretion product.

Due to the importance of antimicrobial activity in tick egg wax coat, GO proteome analysis was further refined to search for antimicrobial peptides (Supplementary Fig. 2). The antimicrobial peptide microplusin (Fogaça et al., 2004) was detected in GO during oviposition. This peptide has antimicrobial activity against the Gram-positive *Micrococcus luteus*, as well as yeasts (Esteves et al., 2009; Silva et al., 2009). Microplusin was identified in *R. microplus* egg homogenates and ovary yolk granules, suggesting its presence inside the egg; however, the peptide was not detected on egg surface (Esteves et al., 2009). There is so far no evidence that microplusin is secreted by GO onto the egg surface, however its antimicrobial activity could also be important for GO itself, since the organ is exposed to the environment during wax secretion. A second antimicrobial peptide detected in GO before and

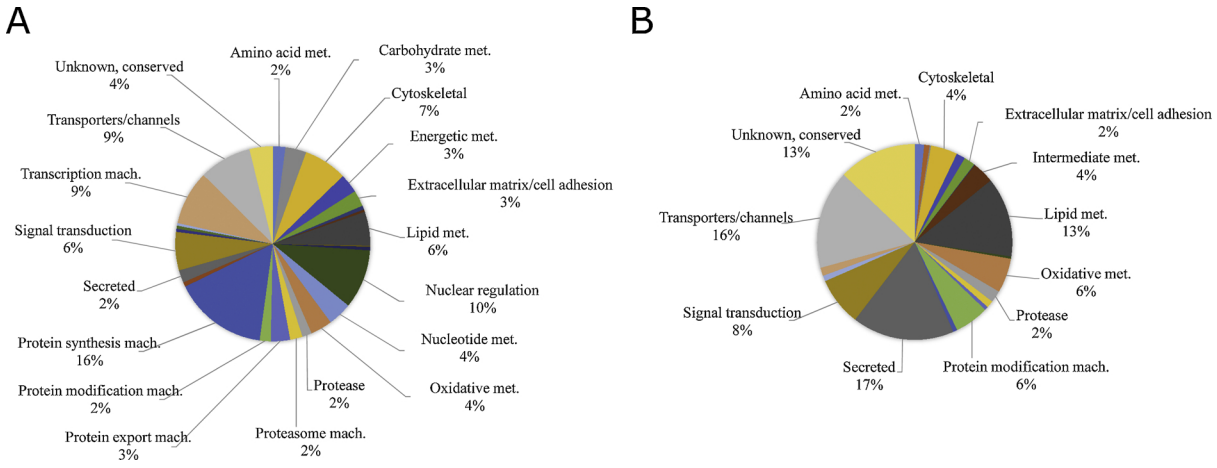

Fig. 3. Proteins exclusively present in Gené's organ (GO) before or during egg-laying. Protein was obtained from GO in two developmental stages: (A) within 24 h of detachment from host (DET group) and (B) in the second day of oviposition (OVP group), i.e. around 5 days after detachment. Pie chart displays proteins exclusively identified in one of the groups (see Fig. 2A). Identified proteins are categorized according to their biological function. Categories' NSAF (Normalized Spectral Abundance Factor) is presented as percentage, normalized by the total NSAF of each group, in order to represent the total amount of each category in each GO stage. mach = machinery; met = metabolism.

Table 4
Proteins involved in fatty acid metabolism found in GO proteome.

Contig*	Protein	NSAF in DET group	NSAF in OVP group
Rm-6290	Choline-phosphate cytidylyltransferase	0.00	12.95
Rm-13823	Ethanolamine-phosphate cytidylyltransferase	0.00	7.34
	Fatty acid synthesis		
RmGO-3714	Fatty acid synthase	4.79	0.00
RmGO-4059	Fatty acid synthase	16.15	5.06
Rm-23018	Acyl carrier protein	10.21	46.57
Rm-42231	Cyclopropane fatty acid synthase	2.71	0.00
Rm-4764	Stearoyl-CoA desaturase	19.35	73.50
	Fatty acid elongation		
Rm-68739	Elongation of VLFA protein	23.50	0.00
Rm-72608	Elongation of VLFA (similar to steroid reductase)	51.87	10.85
Rm-72609	Elongation of VLFA (similar to steroid reductase)	69.43	13.36
Rm-123996	Elongation of VLFA protein	0.00	39.66
Rm-102163	Elongation of VLFA protein 4	5.10	0.00
Rm-141551	Fatty acyl-CoA elongase	2.50	0.00
Rm-33279	Fatty acyl-CoA elongase	14.79	7.12
Rm-9802	Fatty acyl-CoA elongase	14.10	17.11
Rm-4369	3-hydroxyacyl-CoA dehydratase	16.39	0.00
Rm-96077	Acyl-CoA binding domain	9.64	4.42
Rm-96078	Acyl-CoA-binding domain-containing protein	11.08	18.37
Rm-49202	Acyl-CoA-binding protein	231.16	679.98
	Fatty acid oxidation		
Rm-31646	Acyl-CoA synthetase	5.00	0.00
Rm-41707	Acyl-CoA synthetase	2.04	0.00
Rm-11272	Long-chain acyl-CoA synthetase	19.07	0.00
Rm-32430	Acyl-CoA synthetase family member 2	0.00	1.83
Rm-25620	Acyl-CoA synthetase	23.82	2.31
Rm-144805	Acyl-CoA synthetase family member	0.00	19.82
RmGO-4794	Acetyl-coenzyme A synthetase, cytoplasmic	34.24	62.07
RmGO-6325	Acyl-CoA synthetase short-chain family member 2	22.16	105.62
RmGO-6254	Acyl-CoA synthetase short-chain family member 2	44.08	107.67
Rm-16734	Carnitine O-palmitoyltransferase 1	2.93	0.00
Rm-18519	Carnitine O-palmitoyltransferase 2	11.37	13.08
Rm-119479	Citronellyl-CoA dehydrogenase	1.30	0.00
Rm-13248	Isovaleryl-CoA dehydrogenase	8.47	0.00
Rm-22359	Very long chain acyl-CoA dehydrogenase	38.78	17.94
Rm-61015	Butyryl-CoA dehydrogenase	13.27	1.78
Rm-25417	Isobutyryl-CoA dehydrogenase	16.25	14.68
Rm-56723	Acyl-CoA dehydrogenase	47.77	61.62
Rm-55835	Enoyl-CoA hydratase	99.47	40.60
Rm-33595	Enoyl-CoA hydratase / long-chain 3-hydroxyacyl-CoA dehydrogenase	245.01	306.54
Rm-19009	Enoyl-CoA hydratase	36.32	26.85
Rm-32779	Enoyl-CoA hydratase / long-chain 3-hydroxyacyl-CoA dehydrogenase	272.07	326.66
Rm-78641	3-hydroxyacyl-CoA dehydrogenase	35.89	25.34
Rm-26374	3-hydroxyacyl-CoA dehydrogenase/ 3a,7a,12a-trihydroxy-5b-cholest-24-enoyl-CoA hydratase	147.42	216.44
Rm-50647	Acetyl-CoA C-acetyltransferase	43.86	85.12
Rm-75624	3-ketoacyl-CoA thiolase	75.15	129.17
Rm-25655	3-ketoacyl-CoA thiolase	24.97	46.40

* Contig = sequence name in current GO proteome.

during egg-laying is an ixodidin-like peptide. Ixodidin has antimicrobial activity against *M. luteus* and *Escherichia coli*, and inhibits chymotrypsin and elastase (Fogaça et al., 2006). Whether an ixodidin-like peptide would function in GO as an antimicrobial or as a protease inhibitor remains to be elucidated.

3.3. Gené's organ synthesize, modify and oxidize lipids

The importance of GO was described by Gené in 1848 and Bertkau in 1881, but the first evidence suggesting its secretion product is mainly composed by lipids came a century later (Lees and Beament, 1948). Histological observations support the idea that GO has a role in wax secretion and also in its synthesis, due to an enrichment of smooth and rough endoplasmic reticulum, Golgi, mitochondria, and lipid droplets in the cytoplasm of GO secretory cells (Booth, 1989; dos Santos et al., 2018; Kakuda et al., 1995). This conclusion is corroborated by the present data showing the presence of enzymes and other proteins involved in lipid metabolism before and during egg-laying (Fig. 2B), with higher abundance during oviposition (Fig. 3).

Proteins implicated in lipid metabolism that were exclusively found before egg-laying are related to fatty acid biosynthesis, activation, elongation and oxidation, biosynthesis and degradation of phospholipids and cholesterol transport. In contrast, proteins exclusively present during oviposition are involved in fatty acid activation, elongation and oxidation, isoprenoid biosynthesis, modification and degradation of cholesterol esters. Among the proteins exclusively present during oviposition we identified phosphocholine- and phosphoethanolamine cytidylyltransferases (Table 4); the two enzymes participate in the main pathways for the *de novo* synthesis of phosphocholine and phosphoethanolamine, respectively (Gibellini and Smith, 2010). These are major glycerophospholipids present in eukaryotic cell membranes (Lagace and Ridgway, 2013), and are also present in egg wax, although at a lower abundance relative to other lipids (Yu et al., 2012).

Among lipid metabolism proteins found in common, but quantitatively different between the two stages (Fig. 2C), proteins involved in fatty acid elongation and oxidation, lipid transport and steroid metabolism predominate before the onset of oviposition. On the other hand, during oviposition, proteins related to fatty acid biosynthesis, activation and oxidation, acyl-CoA binding proteins (ACBP), and sterol metabolism are more abundant. Altogether, these data indicate that GO role in lipid metabolism before egg-laying favors fatty acid and steroid metabolism and transport, while during oviposition, fatty acid metabolism is maintained, but steroid modification and degradation increase. Indeed, a higher abundance of vitellogenins is detected before egg-laying, namely vitellogenin 2 and 5, which transport lipids from fat body to other organs (Kluck et al., 2018).

3.3.1. Fatty acid metabolism in Gené's organ

GO proteomic data show the presence of fatty acid synthases and their associated protein, acyl-carrier protein, before and during egg-laying (Table 4). Additionally, stearoyl-CoA desaturase and, interestingly, the less common cyclopropane fatty acid synthase are also present (Table 4). These enzymes participate in fatty acid biosynthesis by introducing unsaturation and by inserting a propane, respectively. Also, enzymes participating in the four-step process of fatty acid elongation (Kihara, 2012) are present before and during egg-laying (Table 4).

Acyl-CoA binding domain-containing proteins (ACBP) are known to function as intracellular acyl-CoA transporters, and to be involved in fatty acid elongation and sphingolipid synthesis (Neess et al., 2015). The presence of ACBP was detected at both GO developmental stages, being more pronounced during egg-laying (Table 4).

Among proteins related to fatty acid oxidation, acyl-CoA synthetases are present at both developmental stages, but more conspicuously during egg-laying (Table 4 and Fig. 4A). Carnitine palmitoyltransferase-1 and -2 are also present at both stages; however, carnitine-acylcarnitine translocase was not found (Table 4 and Fig. 4A). Enzymes catalyzing mitochondrial β-oxidation of saturated fatty acid (oxidation, hydration, oxidation, and thiolysis) (Adeva-Andany et al., 2018) are all present in GO, before and during oviposition (Table 4 and Fig. 4B).

3.3.2. Steroids metabolism in Gené's organ

Similar to insects (CLARK and BLOCK, 1959), ticks are unable to synthesize the steroidal ring (Maroun and Kamal, 1976). Nevertheless, steroids derivatives are present and have crucial roles in tick metabolism, e.g. molting hormones (ecdysteroids and sesquiterpenoids) (Qu

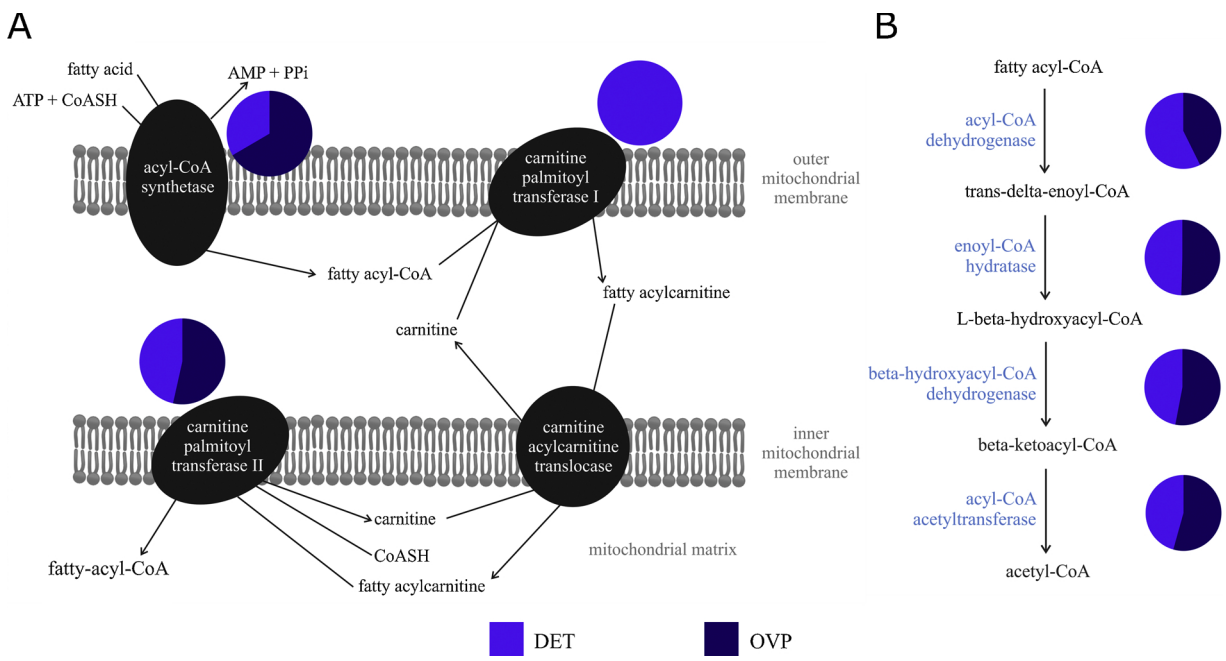

Fig. 4. Fatty acid β-oxidation enzymes present in Gené's organ (GO) proteome. (A) The L-carnitine pathway to transport long- and medium-chain fatty acyl-CoA esters across the mitochondrial membrane. (B) Reaction steps involved in the β-oxidation of fatty acyl-CoA esters. Pie charts next to the enzymes display protein abundance in DET and/or OVP groups. DET group comprises ticks within 24 h of detachment from host, while OVP group is formed by ticks in the second day of oviposition, i.e. around 5 days after detachment.

et al., 2015), and free cholesterol and cholesterol esters in egg wax (Yu et al., 2012).

Mevalonate pathway exists in all higher eukaryotes and many bacteria. The importance of this pathway comes from its involvement in multiple metabolic functions, such as cholesterol synthesis and protein prenylation (Bellös et al., 2005; Glomset et al., 1990). Enzymes from mevalonate pathway related to prenylation are present in GO (highlighted in blue in Fig. 5), while enzymes participating in cholesterol synthesis were not found, in agreement with the notion that ticks do not synthesize cholesterol *de novo* (Maroun and Kamal, 1976). Likewise, enzymes from mevalonate pathway involved in steroid synthesis were not found in tick synganglion transcriptome (Zhu et al., 2016).

Other enzymes involved in steroid metabolism were detected in GO (Table 5), including hydroxysteroid dehydrogenases (HSDs; 3β-HSD, 17β-HSD, HSD like protein 2), which in mammals are involved in modifying or processing the steroidal ring (Penning, 1997). Oxidoreductases acting upon sterols (Penning, 1997) were also present: dehydrogenase/reductase 4, belonging to the short-chain dehydrogenases/reductases family, and 20-HSDs. Since ticks do not synthesize sterols *de novo*, these sterol metabolism enzymes may be involved in modifying exogenous sterols, originated from the host.

A cholesterol desaturase (DAF-36) is present in GO proteome, at higher abundance during egg-laying (Table 5). This protein may convert cholesterol into bioactive steroids, similar to its role in *Caenorhabditis elegans* (Wollam et al., 2011). Vigilin, an RNA-binding protein, regulates apolipoprotein B (apoB), apoC-III and fibronectin translation, and VLDL secretion, regulating triglyceride secretion in murine liver (Mobin et al., 2016). In GO, vigilin is more abundant before egg-laying (Table 5), and may be involved in the regulation of lipid secretion, given that up-regulation of murine vigilin leads to enhanced apoB synthesis and VLDL secretion when lipid availability is increased (Mobin et al., 2016). Oxysterol-binding proteins (OSBP) are present in GO before and during egg-laying (Table 5). OSBP and related proteins (ORP) are involved in cellular processes of signaling, vesicular trafficking, lipid metabolism, and non-vesicular sterol transfer (Olkkonen and Li, 2013; Raychaudhuri and Prinz, 2010).

A lipoprotein circulating in *R. microplus* hemolymph, namely HeLp (heme lipoprotein) (Maya-Monteiro et al., 2000), is also present in GO at both developmental stages, more abundantly before egg-laying. HeLp is a hemeglycolipoprotein, with cholesterol ester reaching 35% of total lipid content (Maya-Monteiro et al., 2000). It is likely that HeLp carries lipids derived from fat body or diet to GO. Another protein involved in cholesterol metabolism is Niemann Pick C1-like protein (NPC1), which plays an essential role in lipid absorption in mammals (Altmann et al., 2004). It is also present at both developmental stages of GO and is more abundant during egg-laying. In *Drosophila melanogaster*, a mutation in *npc1b* gene led to poor cholesterol absorption in the gut, which was not observed in *npc1a* mutants or *npc1a/npc1b* double mutants, suggesting that, at least in this arthropod, there is an alternative pathway for cholesterol absorption (Voght et al., 2007).

Related to sterol catabolism, a methylmalonyl-CoA mutase was detected before and during egg-laying (Table 5). This enzyme directs the breakdown of some amino acids, odd-chain fatty acids, and the side chain of cholesterol, to the tricarboxylic acid cycle (Forny et al., 2014). Additionally, a lysosomal acid lipase/cholesteryl ester hydrolase, which hydrolyses cholesterol esters to free cholesterol, is present in GO during oviposition. After leaving the lysosome, free cholesterol is re-esterified in the endoplasmic reticulum, in order to form lipid droplets (Dubland and Francis, 2015).

Altogether, our results support the hypothesis that GO is equipped with the full machinery for synthesis, elongation, oxidation, and secretion of fatty acids; it also has a machinery for modification, degradation, and secretion of sterols, despite not being able to synthesize them. Lipid secretion is performed by GO secretory glands, in order to cover the eggs and protect them from environmental conditions of humidity and temperature, and from microorganisms. Proteomic and transcriptomic data reveal that, before egg-laying, GO is engaged in preparation for its role during oviposition, as suggested by the presence of cell division machinery, transcription and protein synthesis, including proteins that participate in cytoskeleton composition. Protein synthesis is maintained in the next stage during egg-laying, while the secretion, transport, and metabolism of wax content is more abundant, in order to coat the huge number of eggs each tick lays. To date, a few reports on GO focused on morphology, histology, *modus operandi*, and

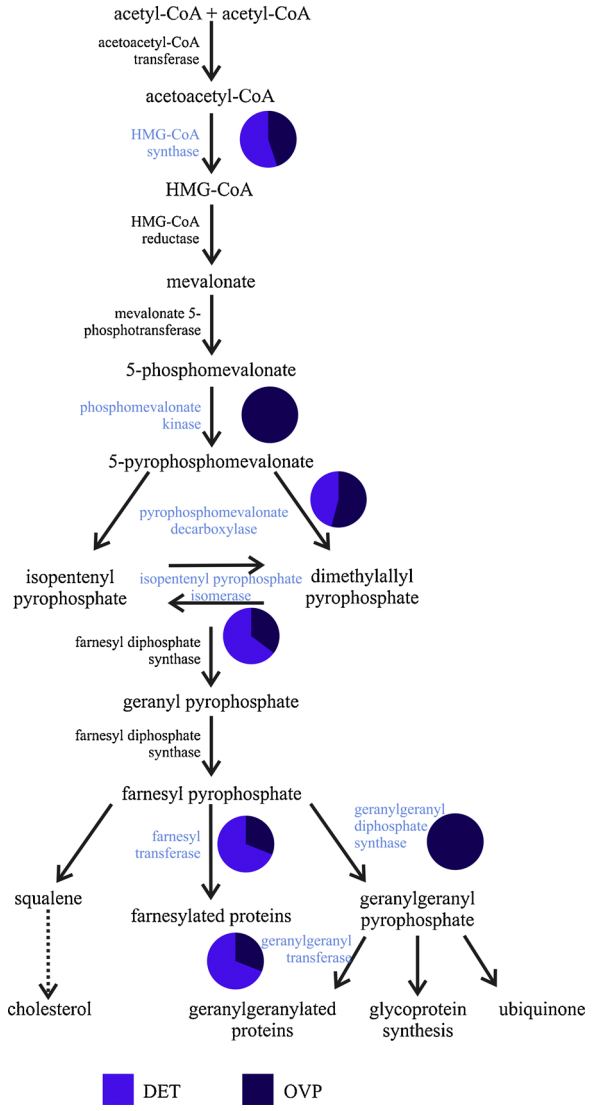

Fig. 5. Mevalonate pathway enzymes present in Gené's organ (GO) proteome. Enzymes from mevalonate pathway identified in GO proteome are highlighted in blue. Next to each enzyme, pie charts display protein abundance in DET and/or OVP groups. (For interpretation of the references to colour in this figure legend, the reader is referred to the web version of this article).
DET group comprises ticks within 24 h of detachment from host, while OVP group is formed by ticks in the second day of oviposition, i.e. around 5 days after detachment.

wax lipid composition. The present study offers a new insight into GO physiology, showing metabolic pathways that are present during the maturation of this organ, and highlighting its importance in tick reproduction. Furthermore, this kind of approach unveils proteins and pathways contributing to egg viability and development in the environment, thus identifying potential targets for new tick control methods.

4. Author contributions

Conceived and designed the experiments: M.A.X., L.T., A.F.M.P., S.G., M.F., I.S.V.J. and C.T.

Performed the experiments: M.A.X., L.T., A.F.M.P., J.K.D., and S.G.

Contributed reagents/materials/analysis tools: J.R.Y., M.F., I.S.V.J., and C.T.

Drafting the article: M.A.X., L.T., A.F.M.P., I.S.V.J. and C.T.

Critical revision of the article: M.A.X., L.T., A.F.M.P., J.K.D., J.R.Y., S.G., M.F., I.S.V.J., and C.T.

Table 5
Proteins related to sterol metabolism found in GO proteome.

Contig*	Protein	NSAF in DET group	NSAF in OVP group
	Hydroxysteroid dehydrogenases (HSDs)		
Rm-17271	C-3 sterol dehydrogenase/3-beta-hydroxysteroid dehydrogenase	27.87	4.17
Rm-27216	17 beta-estradiol 17-dehydrogenase / very-long-chain 3-oxoacyl-CoA reductase	142.83	94.69
Rm-27217	17 beta-estradiol 17-dehydrogenase / very-long-chain 3-oxoacyl-CoA reductase	161.81	108.26
Rm-24527	Hydroxysteroid dehydrogenase like protein 2	11.43	10.81
	Oxidoreductases		
Rm-17111	Dehydrogenase/reductase SDR family member 4	14.13	25.95
Rm-20284	20-hydroxysteroid dehydrogenase	89.76	64.52
Rm-44374	20-hydroxysteroid dehydrogenase	91.60	68.64
Rm-74118	20-hydroxysteroid dehydrogenase	66.89	56.19
	Cholesterol metabolism		
Rm-76179	Cholesterol desaturase daf-36	0.00	6.74
RmGO-5901	Cholesterol desaturase daf-36	0.00	40.45
	Lipid secretion regulation		
Rm-120182	Vigilin	19.63	3.97
	Oxysterol and cholesterol-binding		
Rm-46794	Oxysterol-binding protein	16.82	37.85
Rm-19473	Oxysterol-binding protein	8.32	4.03
	Lipoprotein		
Rm-6525	Hemelipoprotein (HeLp)	84.17	5.08
Rm-89257	Hemelipoprotein (HeLp) 2	109.32	5.41
	Lipid absorption		
Rm-32890	Niemann-Pick C1 protein	8.66	0.00
Rm-74103	Niemann-Pick C1 protein	119.50	219.01
Rm-57573	Niemann-Pick C2 protein	59.99	111.66
Rm-18926	Niemann-Pick C2 protein	0.00	24.52
	Sterol catabolism		
Rm-71018	Methylmalonyl-CoA mutase	21.59	11.44
Rm-70838	Methylmalonyl-CoA mutase	20.16	8.78
Rm-7892	Lysosomal acid lipase/cholesteryl ester hydrolase	0.00	34.40

* Contig = sequence name in current GO proteome.

Conflict of interest

The authors certify that they have no affiliations with, or involvement in any organization or entity with any financial interest in the subject matter or materials discussed in this manuscript.

Acknowledgements

This research was supported by FAPERJ, INCT-Entomologia Molecular, CNPq and CAPES from Brazil; by CONICET from Argentina; by National Institute of General Medical Sciences (8 P41 GM103533) from USA. The authors would like to thank Dr. José M.C. Ribeiro for providing the VB programs used in transcriptomic analysis and protein annotation.

Appendix A. Supplementary data

Supplementary data associated with this article can be found, in the online version, at https://doi.org/10.1016/j.ttbdis.2019.03.013.

References

Adeva-Andany, M.M., Carneiro-Freire, N., Seco-Filgueira, M., Fernández-Fernández, C., Mouriño-Bayolo, D., 2018. Mitochondrial β-oxidation of saturated fatty acids in

humans. Mitochondrion 1–18. https://doi.org/10.1016/j.mito.2018.02.009.
Altmann, S.W., Davis, H.R., Zhu, L.J., Yao, X., Hoos, L.M., Tetzloff, G., Iyer, S.P.N., Maguire, M., Golovko, A., Zeng, M., Wang, L., Murgolo, N., Graziano, M.P., 2004. Niemann-Pick C1 Like 1 Protein is critical for intestinal cholesterol absorption. Science 303, 1201–1204. https://doi.org/10.1126/science.1093131.
Altschul, S.F., Madden, T.L., Schäffer, A.A., Zhang, J., Zhang, Z., Miller, W., Lipman, D.J., 1997. Gapped BLAST and PSI-BLAST: a new generation of protein database search programs. Nucleic Acids Res. 25, 3389–3402. https://doi.org/10.1093/nar/25.17.3389.
Arrese, E.L., Soulages, J.L., 2010. Insect fat body: energy, metabolism, and regulation. Annu. Rev. Entomol. 55, 207–225. https://doi.org/10.1146/annurev-ento-112408-085356.
Arrieta, M.C., Leskiw, B.K., Kaufman, W.R., 2006. Antimicrobial activity in the egg wax of the African cattle tick *Amblyomma hebraeum*(Acari: Ixodidae). Exp. Appl. Acarol. 39, 297–313. https://doi.org/10.1007/s10493-006-9014-5.
Beaufays, J., Adam, B., Decrem, Y., Prévôt, P.P., Santini, S., Brasseur, R., Brossard, M., Lins, L., Vanhamme, L., Godfroid, E., 2008. *Ixodes ricinus* tick lipocalins: identifications, cloning, phylogenetic analysis and biochemical characterization. PLoS ONE 3, e3941. https://doi.org/10.1371/journal.pone.0003941.
Bellés, X., Martín, D., Piulachs, M.-D., 2005. The mevalonate pathway and the synthesis of juvenile hormone in insects. Annu. Rev. Entomol. 50, 181–199. https://doi.org/10.1146/annurev.ento.50.071803.130356.
Bolger, A.M., Lohse, M., Usadel, B., 2014. Trimmomatic: A flexible trimmer for Illumina sequence data. Bioinformatics 30, 2114–2120. https://doi.org/10.1093/bioinformatics/btu170.
Booth, T.F., 1989. Wax lipid secretion and ultrastructural development in the egg-waxing (Gené's) organ in ixodid ticks. Tissue Cell 21, 113–122. https://doi.org/10.1016/0040-8166(89)90026-8.
Booth, T.F., 1992. Observation on the composition and biosynthesis of egg wax lipids in the cattle tick, *Boophilus microplus*. Exp. Appl. Acarol. 14, 137–149. https://doi.org/10.1007/BF01219106.
Booth, T.F., Beadle, D.J., Hart, R.J., 1985. An ultrastructural and physiological investigation of the retractor muscles of Gené's organ in the cattle ticks *Boophilus microplus* and *Amblyomma variegatum*. Exp. Appl. Acarol. 1, 165–177. https://doi.org/10.1007/BF01270595.
Canavoso, L.E., Jouni, Z.E., Karnas, K.J., Pennington, J.E., Wells, M.A., 2001. Fat metabolism in insects. Annu. Rev. Nutr. 21, 23–46. https://doi.org/10.1146/annurev.nutr.21.1.23.
Carvalho, P.C., Lima, D.B., Leprevost, F.V., Santos, M.D.M., Fischer, J.S.G., Aquino, P.F., Moresco, J.J., Yates, J.R., Barbosa, V.C., 2016. Integrated analysis of shotgun proteomic data with PatternLab for proteomics 4.0. Nat. Protoc 11, 102–117. https://doi.org/10.1038/nprot.2015.133.
Clark, A.J., Block, K., 1959. The absence of sterol synthesis in insects. J. Biol. Chem. 234, 2578–2582.
De Lima-Netto, S., Pinheiro, A., Nakano, E., Zucatelli Mendonça, R.M., Barros-Battesti, D.M., Mendonça, R.Z., 2012. Antiviral effect of the egg wax of *Amblyomma cajennense* (Acari: Ixodidae). Cytotechnology 64, 601–606. https://doi.org/10.1007/s10616-012-9444-3.
Deutsch, E.W., Csordas, A., Sun, Z., Jarnuczak, A., Perez-Riverol, Y., Ternent, T., Campbell, D.S., Bernal-Llinares, M., Okuda, S., Kawano, S., Moritz, R.L., Carver, J.J., Wang, M., Ishihama, Y., Bandeira, N., Hermjakob, H., Vizcaíno, J.A., 2017. The ProteomeXchange consortium in 2017: supporting the cultural change in proteomics public data deposition. Nucleic Acids Res. 45, D1100–D1106. https://doi.org/10.1093/nar/gkw936.
dos Santos, M.F., Maltauro Soares, M.A., Lallo, M.A., Barros-Battesti, D.M., de Lima-Netto, S., Spadacci-Morena, D.D., 2018. Morphodifferentiation of Gené's organ in engorged*Amblyomma sculptum* Berlese, 1888 female ticks (Acari: Ixodidae). Ticks Tick. Dis. 9, 519–525. https://doi.org/10.1016/j.ttbdis.2018.01.004.
Dubland, J.A., Francis, G.A., 2015. Lysosomal acid lipase: at the crossroads of normal and atherogenic cholesterol metabolism. Front. Cell Dev. Biol. 3, 1–11. https://doi.org/10.3389/fcell.2015.00003.
Edelmann, B., Gothe, R., 2000. The mechanism of oviposition in *Argas (Persicargas) walkerae*(Acari: Argasidae). Exp. Appl. Acarol. 24, 927–940. https://doi.org/10.1023/A:1010613202269.
El Shoura, S.M., 1987. Fine structure of the Gene's organ in the camel tick *Hyalomma (Hyalomma) dromedarii*(Ixodoidea: Ixodidae). J. Morphol. 193, 91–98. https://doi.org/10.1007/BF01197927.
El Shoura, S.M., 1988. Fine structure of the vagina, accessory glands, uterus, oviducts and Gene's organ in the unfed tick, *Ornithodoros (Pavlovskyella) erraticus*(Ixodoidea: Argasidae). Exp. Appl. Acarol. 4, 95–108. https://doi.org/10.1007/BF01193868.
Eng, J.K., Jahan, T.A., Hoopmann, M.R., 2013. Comet: an open-source MS/MS sequence database search tool. Proteomics 13, 22–24. https://doi.org/10.1002/pmic.201200439.
Esteves, E., Fogaça, A.C., Maldonado, R., Silva, F.D., Manso, P.P.A., Pelajo-Machado, M., Valle, D., Daffre, S., 2009. Antimicrobial activity in the tick *Rhipicephalus (Boophilus) microplus* eggs: cellular localization and temporal expression of microplusin during oogenesis and embryogenesis. Dev. Comp. Immunol. 33, 913–919. https://doi.org/10.1016/j.dci.2009.02.009.
Fogaça, A.C., Lorenzini, D.M., Kaku, L.M., Esteves, E., Bulet, P., Daffre, S., 2004. Cysteine-rich antimicrobial peptides of the cattle tick *Boophilus microplus*: isolation, structural characterization and tissue expression profile. Dev. Comp. Immunol. 28, 191–200. https://doi.org/10.1016/j.dci.2003.08.001.
Fogaça, A.C., Almeida, I.C., Eberlin, M.N., Tanaka, A.S., Bulet, P., Daffre, S., 2006. Ixodidin, a novel antimicrobial peptide from the hemocytes of the cattle tick *Boophilus microplus* with inhibitory activity against serine proteinases. Peptides 27, 667–674. https://doi.org/10.1016/j.peptides.2005.07.013.
Forny, P., Froese, D.S., Suormala, T., Yue, W.W., Baumgartner, M.R., 2014. Functional characterization and categorization of missense mutations that cause methylmalonyl-CoA mutase (MUT) deficiency. Hum. Mutat. 35, 1449–1458. https://doi.org/10.1002/humu.22633.
Gibellini, F., Smith, T.K., 2010. The Kennedy pathway-*de novo* synthesis of phosphatidylethanolamine and phosphatidylcholine. IUBMB Life 62, 414–428. https://doi.org/10.1002/iub.337.
Glomset, J.A., Gelb, M.H., Farnsworth, C.C., 1990. Prenyl proteins in eukaryotic cells: a new type of membrane anchor. Trends Biochem. Sci. 15, 139–142. https://doi.org/10.1016/0968-0004(90)90213-U.
Grabherr, M.G., Haas, B.J., Yassour, M., Levin, J.Z., Thompson, D.A., Amit, I., Adiconis, X., Fan, L., Raychowdhury, R., Zeng, Q., Chen, Z., Mauceli, E., Hacohen, N., Gnirke, A., Rhind, N., Di Palma, F., Birren, B.W., Nusbaum, C., Lindblad-Toh, K., Friedman, N., Regev, A., 2011. Full-length transcriptome assembly from RNA-Seq data without a reference genome. Nat. Biotechnol. 29, 644–652. https://doi.org/10.1038/nbt.1883.
Kakuda, H., Mori, T., Shiraishi, S., 1992. Functional morphology of Gené's organ in*Haemaphysalis longicornis* (Acari: Ixodidae). Exp. Appl. Acarol. 16, 263–275. https://doi.org/10.1007/BF01193809.
Kakuda, H., Nishimura, H., Mari, T., Shiraishi, S., 1995. Structural changes of the female genital system during and after feeding in *Haemaphysalis longicornis*(Acari: Ixodidae). J. Fac. Agric. - Kyushu Univ. 40, 61–71.
Karim, S., Singh, P., Ribeiro, J.M.C., 2011. A deep insight into the sialotranscriptome of the gulf coast tick, *Amblyomma maculatum*. PLoS One 6, e28525. https://doi.org/10.1371/journal.pone.0028525.
Kihara, A., 2012. Very long-chain fatty acids: elongation, physiology and related disorders. J. Biochem. 152, 387–395. https://doi.org/10.1093/jb/mvs105.
Kluck, G.E.G., Silva Cardoso, L., De Cicco, N.N.T., Lima, M.S., Folly, E., Atella, G.C., 2018. A new lipid carrier protein in the cattle tick *Rhipicephalus microplus*. Ticks Tick. Dis. 9, 850–859. https://doi.org/10.1016/j.ttbdis.2018.03.010.
Lagace, T.A., Ridgway, N.D., 2013. The role of phospholipids in the biological activity and structure of the endoplasmic reticulum. Biochim. Biophys. Acta - Mol. Cell Res. 1833, 2499–2510. https://doi.org/10.1016/j.bbamcr.2013.05.018.
Langmead, B., Salzberg, S.L., 2012. Fast gapped-read alignment with Bowtie 2. Nat. Methods 9, 357–359. https://doi.org/10.1038/nmeth.1923.
Lees, A.D., Beament, J.W.L., 1948. An egg-waxing organ in ticks. Q. J. Microsc. Sci. 89, 291–322.
Magoč, T., Salzberg, S.L., 2011. FLASH: fast length adjustment of short reads to improve genome assemblies. Bioinformatics 27, 2957–2963. https://doi.org/10.1093/bioinformatics/btr507.
Majerowicz, D., Gondim, K.C., 2013. Insect lipid metabolism: insights into gene expression regulation. In book: recent trends in Gene expression, edition 1, chapter 7. Recent Trends in Gene Expression. pp. 147–190.
Marchler-Bauer, A., Panchenko, A.R., Shoemarker, B.A., Thiessen, P.A., Geer, L.Y., Bryant, S.H., 2002. CDD: a database of conserved domain alignments with links to domain three-dimensional structure. Nucleic Acids Res. 30, 281–283. https://doi.org/10.1093/nar/30.1.281.
Maroun, N.A., Kamal, K.A., 1976. Biochemical and physiological studies of certain ticks (Ixodoidea). Absence of sterol biosynthesis in*Dermacentor andersoni stiles* (Acarina: Ixodidae). J. Med. Entomol. 13, 219–220. https://doi.org/10.1093/jmedent/13.2.219.
Maya-Monteiro, C.M., Daffre, S., Logullo, C., Lara, F.A., Alves, E.W., Capurro, M.L., Zingali, R., Almeida, I.C., Oliveira, P.L., 2000. HeLp, a heme lipoprotein from the hemolymph of the cattle tick, *Boophilus microplus*. J. Biol. Chem. 275, 36584–36589. https://doi.org/10.1074/jbc.M007344200.
Mobin, M.B., Gerstberger, S., Teupser, D., Campana, B., Charisse, K., Heim, M.H., Manoharan, M., Tuschl, T., Stoffel, M., 2016. The RNA-binding protein vigilin regulates VLDL secretion through modulation of Apob mRNA translation. Nat. Commun. 7, 12848. https://doi.org/10.1038/ncomms12848.
Neelakanta, G., Sultana, H., Sonenshine, D.E., Andersen, J.F., 2018. Identification and characterization of a histamine-binding lipocalin-like molecule from the relapsing fever tick *Ornithodoros turicata*. Insect Mol. Biol. 27, 177–187. https://doi.org/10.1111/imb.12362.
Neess, D., Bek, S., Engelsby, H., Gallego, S.F., Færgeman, N.J., 2015. Long-chain acyl-CoA esters in metabolism and signaling: role of acyl-CoA binding proteins. Prog. Lipid Res. 59, 1–25. https://doi.org/10.1016/j.plipres.2015.04.001.
Olkkonen, V.M., Li, S., 2013. Oxysterol-binding proteins: sterol and phosphoinositide sensors coordinating transport, signaling and metabolism. Prog. Lipid Res. 52, 529–538. https://doi.org/10.1016/j.plipres.2013.06.004.
Penning, T.M., 1997. Molecular endocrinology of hydroxysteroid dehydrogenases. Endocr. Rev. 18, 281–305. https://doi.org/10.1016/j.adaj.2014.12.008.
Potterat, O., Hostettmann, K., Hölzel, A., Jung, G., Diehl, P.A., Petrini, O., 1997. Boophiline, an antimicrobial sterol amide from the cattle tick *Boophilus microplus*. Helv. Chim. Acta 80, 2066–2072. https://doi.org/10.1002/hlca.19970800707.
Qu, Z., Kenny, N.J., Lam, H.M., Chan, T.F., Chu, K.H., Bendena, W.G., Tobe, S.S., Hui, J.H.L., 2015. How did arthropod sesquiterpenoids and ecdysteroids arise? Comparison of hormonal pathway genes in noninsect arthropod genomes. Genome Biol. Evol. 7, 1951–1959. https://doi.org/10.1093/gbe/evv120.
Raychaudhuri, S., Prinz, W.A., 2010. The diverse functions of oxysterol-binding proteins. Annu. Rev. Cell Dev. Biol. 26, 157–177. https://doi.org/10.1146/annurev.cellbio.042308.113334.
Reck, J., Berger, M., Terra, R.M.S., Marks, F.S., da Silva Vaz, I., Guimarães, J.A., Termignoni, C., 2009. Systemic alterations of bovine hemostasis due to *Rhipicephalus (Boophilus) microplus* infestation. Res. Vet. Sci. 86, 56–62. https://doi.org/10.1016/j.rvsc.2008.05.007.
Ribeiro, J.M.C., Martin-Martin, I., Arcá, B., Calvo, E., 2016. A deep insight into the sialome of male and female *Aedes aegypti* mosquitoes. PLoS One 11, e0151400. https://

doi.org/10.1371/journal.pone.0151400.
Roberts, A., Pachter, L., 2013. Streaming fragment assignment for real-time analysis of sequencing experiments. Nat. Methods 10, 71–73. https://doi.org/10.1038/nmeth.2251.
Robinson, M.D., McCarthy, D.J., Smyth, G.K., 2009. edgeR: A Bioconductor package for differential expression analysis of digital gene expression data. Bioinformatics 26, 139–140. https://doi.org/10.1093/bioinformatics/btp616.
Roversi, P., Johnson, S., Preston, S.G., Nunn, M.A., Paesen, G.C., Austyn, J.M., Nuttall, P.A., Lea, S.M., 2017. Structural basis of cholesterol binding by a novel clade of dendritic cell modulators from ticks. Sci. Rep. 7, 16057. https://doi.org/10.1038/s41598-017-16413-2.
Ryan, R.O., van der Horst, D.J., 2000. Lipid transport biochemistry and its role in energy production. Annu. Rev. Entomol. 45, 233–260. https://doi.org/10.1146/annurev.ento.45.1.233.
Schöl, H., Sieberz, J., Göbel, E., Gothe, R., 2001. Morphology and structural organization of Gené's organ in*Dermacentor reticulatus* (Acari: Ixodidae). Exp. Appl. Acarol. 25, 327–352. https://doi.org/10.1023/A:1017963531560.
Sieberz, J., Gothe, R., 2000. Modus operandi of oviposition in *Dermacentor reticulatus* (Acari: Ixodidae). Exp. Appl. Acarol. 24, 63–76. https://doi.org/10.1023/A:1006351019078.
Silva, F.D., Rezende, C.A., Rossi, D.C.P., Esteves, E., Dyszy, F.H., Schreier, S., Gueiros-Filho, F., Campos, C.B., Pires, J.R., Daffre, S., 2009. Structure and mode of action of microplusin, a copper II-chelating antimicrobial peptide from the cattle tick Rhipicephalus (Boophilus) microplus. J. Biol. Chem. 284, 34735–34746. https://doi.org/10.1074/jbc.M109.016410.
Tidwell, J.T., 2015. Differential Gene Expression Between Two Developmental Stages of the Gené's Organ in the Cattle Fever Tick, Rhipicephalus (Boophilus) Microplus. University of Texas-pan American.
Vizcaíno, J.A., Csordas, A., Del-Toro, N., Dianes, J.A., Griss, J., Lavidas, I., Mayer, G., Perez-Riverol, Y., Reisinger, F., Ternent, T., Xu, Q.W., Wang, R., Hermjakob, H., 2016. 2016 update of the PRIDE database and its related tools. Nucleic Acids Res. 44, D447–D456. https://doi.org/10.1093/nar/gkv1145.
Voght, S.P., Fluegel, M.L., Andrews, L.A., Pallanck, L.J., 2007. Drosophila NPC1b promotes an early step in sterol absorption from the midgut epithelium. Cell Metab. 5, 195–205. https://doi.org/10.1016/j.cmet.2007.01.011.
Wessel, D., Flügge, U.I., 1984. A method for the quantitative recovery of protein in dilute solution in the presence of detergents and lipids. Anal. Biochem. 138, 141–143. https://doi.org/10.1016/0003-2697(84)90782-6.
Wollam, J., Magomedova, L., Magner, D.B., Shen, Y., Rottiers, V., Motola, D.L., Mangelsdorf, D.J., Cummins, C.L., Antebi, A., 2011. The Rieske oxygenase DAF-36 functions as a cholesterol 7-desaturase in steroidogenic pathways governing longevity. Aging Cell 10, 879–884. https://doi.org/10.1111/j.1474-9726.2011.00733.x.
Yu, Z., Thomson, E.L.S., Liu, J., Dennis, J.J., Jacobs, R.L., Kaufman, W.R., 2012. Antimicrobial activity in the egg wax of the tick *Amblyomma hebraeum*(Acari: Ixodidae) is associated with free fatty acids C16:1 and C18:2. Exp. Appl. Acarol. 58, 453–470. https://doi.org/10.1007/s10493-012-9586-1.
Zhu, J., Khalil, S.M., Mitchell, R.D., Bissinger, B.W., Egekwu, N., Sonenshine, D.E., Roe, R.M., 2016. Mevalonate-farnesal biosynthesis in ticks: comparative synganglion transcriptomics and a new perspective. PLoS One 11, 1–27. https://doi.org/10.1371/journal.pone.0141084.
Zimmer, K.R., Macedo, A.J., Giordani, R.B., Conceição, J.M., Nicastro, G.G., Boechat, A.L., Baldini, R.L., Abraham, W.R., Termignoni, C., 2013a. A steroidal molecule present in the egg wax of the tick *Rhipicephalus (Boophilus) microplus* inhibits bacterial biofilms. Environ. Microbiol. 15, 2008–2018. https://doi.org/10.1111/1462-2920.12082.
Zimmer, K.R., Macedo, A.J., Nicastro, G.G., Baldini, R.L., Termignoni, C., 2013b. Egg wax from the cattle tick *Rhipicephalus (Boophilus) microplus* inhibits *Pseudomonas aeruginosa* biofilm. Ticks Tick. Dis. 4, 366–376. https://doi.org/10.1016/j.ttbdis.2013.01.005.
Zybailov, B., Mosley, A.L., Sardiu, M.E., Coleman, M.K., Florens, L., Washburn, M.P., 2006. Statistical analysis of membrane proteome expression changes in Saccharomyces cerevisiae. J. Proteome Res. 5, 2339–2347. https://doi.org/10.1021/pr060161n.